Mechanism of C−H Activation by Diiron Methane Monooxygenases: Quantum Chemical Studies

Per E. M. Siegbahn*,† and Robert H. Crabtree‡

Contribution from the Department of Physics, Stockholm University, Box 6730, S-113 85 Stockholm, Sweden, and Chemistry Department, Yale University, 225 Prospect Street, New Haven, Connecticut, 06520-8107

Received November 13, 1996. Revised Manuscript Received January 27, 1997[⊗]

Abstract: A variety of plausible mechanisms for methane hydroxylation in methane monooxygenases (MMO) have been tested by high-level quantum chemical methods on model systems with simple ligands chosen on the basis of the MMO crystal structure and the available biophysical data. One pathway survives the present level of tests in having intermediates with plausible energies and structures and a low-energy transition state for C−H abstraction. In this proposed pathway, the Fe_2(II,II) dinuclear iron site of the reduced form of MMO reacts with O_2 to give two different Fe_2(III,III) peroxo species and, after O−O bond cleavage, an Fe_2(IV,IV) bis-μ-oxo species probably directly analogous to "compound **Q**" of MMO. As a result of the large Jahn−Teller distortions in the d^4 bis-μ-oxo species, the Fe−O−Fe bridges are highly asymmetric, allowing the system to open up easily to a key Fe^{III}−O−Fe^{V}═O intermediate that is shown to be capable of reacting with methane via a low-energy transition state. This intermediate is shown to be better regarded as having the structure Fe^{III}−O−Fe^{IV}−O$^{\bullet}$, with radical character at the terminal oxo group. After H atom abstraction from methane, the methyl radical recombines very rapidly with the Fe center via a weak Fe−CH_3 bond. With the loss of CH_3OH, an Fe^{III}−O−Fe^{III} dimer is formed that requires reduction to form the Fe_2(II,II) starting species. In addition to the work on the dinuclear species, results on a number of relevant mononuclear Fe(III) and Fe(IV) species are also reported.

I. Introduction

Methane monooxygenases (MMOs) are a group of enzymes which convert methane to methanol via a monooxygenase pathway in which the dioxygen molecule is activated via reduction:[1]

$$CH_4 + O_2 + NADH + H^+ \rightarrow CH_3OH + H_2O + NAD^+ \quad (1)$$

Membrane-bound MMOs containing copper are known,[2] but the longest known MMOs are soluble proteins containing a dinuclear iron active site. The best characterized of these are the proteins from *Methylosinus trichosporium* (OB3b)[3] and *Methylococcus capsulatus* (Bath).[1,4] As methanotrophs, these organisms can use methane as their sole source of carbon and energy. The soluble MMOs consist of three components, a hydroxylase containing the diiron center, a reductase, and the B component. The first interacts with O_2 and then hydroxylates the substrate, the second provides the reducing equivalents called for in eq 1, and the third is believed to mediate electron transfer between the other two components.

The X-ray structure of the 251-kD hydroxylase from *M. capsulatus*,[5] which has recently become available for the oxidized form, shows the dinuclear iron center (d(Fe···Fe) = 3.4 Å) bridged by a hydroxide, a glutamate, and an acetate from the buffer, where waters are expected to be bound in vivo (Figure 1). The terminal ligands are as shown. The identity of the bridging ligand as hydroxyl rather than oxo comes from ENDOR studies.[6] Fe_2(II,II), Fe_2(II,III), and Fe_2(III,III) redox states are accessible, the first of which is believed to react with O_2 to form a peroxo species. In subsequent steps, one of the O atoms of the peroxide is reduced to water and the other is believed to form an iron oxo species of some kind, capable of hydroxylating methane. Without reductase present, the Fe_2(II,II) form of the hydroxylase is capable of carrying out one turnover, implying that the job of the reductase is to recycle the reductase by reduction.

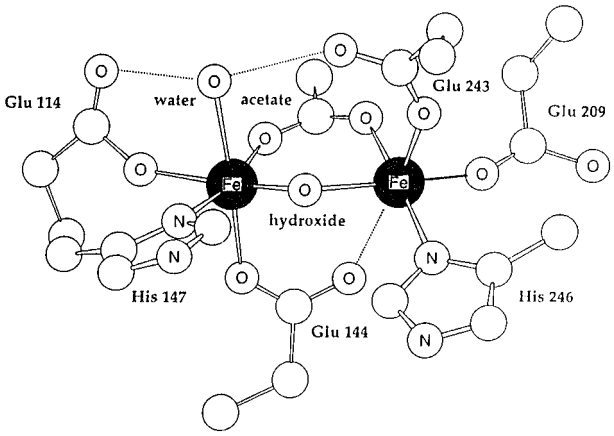

Figure 1. Schematic active site structure of MMO showing the dimeric iron site involved in dioxygen activation and substrate hydroxylation activity. The acetate ligand is an artifact of the isolation technique. (Reproduced from ref 1 by permission of the American Chemical Society.)

† Stockholm University.
‡ Yale University.
[⊗] Abstract published in *Advance ACS Abstracts,* March 15, 1997.

(1) Feig, A. L.; Lippard, S. J. *Chem. Rev.* **1994**, *94*, 759.
(2) Nguyen, H. H. T.; Shiemke, A. K.; Jacobs, S. J.; Hales, B. J.; Lidstrom, M. E.; Chan, S. I. *J. Biol. Chem.* **1994**, *269*, 14995.
(3) (a) Lipscomb, J. D. *Annu. Rev. Microbiol.* **1994**, *48*, 371. (b) Nesheim, J.C.; Lipscomb, J. D. *Biochemistry* **1996**, *35*, 10240 and references cited there. (c) Wallar, B. J.; Lipscomb, J. D. *Chem. Rev.* **1996**, *96*, 2625.
(4) Dalton, H. *Adv. Appl. Microbiol.* **1980**, *26*, 71.
(5) Rosenwieg, A. C.; Frederick, C. A.; Lippard, S. J.; Nordlund, P. *Nature* **1993**, *366*, 537.
(6) (a) Derose, V. J.; Liu, K. E.; Kurtz, D. M.; Hoffman, B. M.; Lippard, S. J. *J. Am. Chem. Soc.* **1993**, *115*, 6440. (b) Thomann, H.; Bernardo, M.; McCormick, J. M.; Pulver, S., Anderssen, K. K.; Lipscomb, J. D.; Solomon, E. I. *J. Am. Chem. Soc.* **1993**, *115*, 8881.

S0002-7863(96)03939-X CCC: $14.00

The chemistry of MMO is reminiscent of the P-450 monooxygenases[7] which contain a heme active site. Methane itself is not attacked by P-450, however, which is only capable of hydroxylating somewhat weaker CH bonds. The mechanism proposed in the P-450 case involves an oxoiron(IV) species with a 1-electron oxidized heme. By analogy, in a nonheme system such as MMO, an Fe_2(IV,IV) oxo might be involved, the oxidizing equivalent assigned to heme in P-450 being associated with the second iron in MMO. Consistent with this proposal, the Fe_2(II,II) form of the hydroxylase gives one turnover with the $4e^-$ oxidant O_2 and the Fe_2(III,III) form of the hydroxylase is weakly catalytically active with H_2O_2 as the two-electron oxidant in the absence of other components.[8] The kinetics and selectivity of the peroxide reaction differ sufficiently from that of the O_2 reaction, however, so that it is still unclear whether the key enzyme intermediates are the same in both cases. Oxo transfer reagents such as PhIO and *t*-BuOOH that are active oxidants in the P-450 system are inactive for MMO, a result that has raised some doubts about the intermediacy of an oxo species,[9] although site accessibility of the hydrophilic substrates to the hydrophobic active site may be limited.

Even so, by analogy with P-450, it is still considered most likely that a high-valent iron oxo intermediate is involved. This might abstract an H atom from the substrate to give a methyl radical which would form methane after abstraction of the resulting OH group from the metal. Strong evidence for the presence of non-heme iron oxo intermediates has also been obtained in model systems.[10−12] For the *M. trichosporium* MMO it has been found that ring-opened products are formed with cyclopropane radical clocks as substrate, consistent with radical (or carbonium ion) intermediates, although the yield of ring-opened products was unexpectedly small.[13]

With chiral ethane (CH_3CHDT) as substrate, 35% inversion of configuration and a deuterium isotope effect (KIE) of 4.2 were observed with *M. trichosporium* MMO.[14] This was interpreted as being most consistent with a substrate radical which is not entirely free but constrained in some way by the enzyme active site. The quantitative interpretation of the data was not entirely consistent with the radical clock studies mentioned above, however, because it required an abnormally short radical lifetime.[1] The intramolecular KIE for *M. trichosporium* MMO (4.2 ± 0.2) was also outside the range found for P-450 enzymes (7−14).[7]

In the *M. capsulatus* case, very fast radical clocks were studied with results inconsistent with the intermediacy of free radical intermediates because the maximum radical lifetime allowed by the data is an unreasonably short 2.5×10^{-4} s.[15] Fast radical clocks with *M. trichosporium* MMO give a small amount of ring-opening products, consistent with a short but not unreasonable radical lifetime of ca. 8×10^{-12} s.

Rapid freeze-quench techniques have allowed a series of intermediates, denoted compounds **O** through **T**, to be identified by Mössbauer spectroscopy[3b] for the *M. trichosporium* enzyme. The key species, compound **Q**, has spectral parameters ($\Delta E_q = 0.53$ mm, $\delta = 0.17$ mm/s) that are most consistent with an Fe_2-(IV,IV) system with indistinguishable irons. The parameters are not far removed from the values found for Fe^{IV}═O hemes and a ferryl intermediate in the model complex of Que et al.[16] Further analysis of the data also shows that compound **Q** is diamagnetic and capable of reaction with hydrocarbons. The review by Feig and Lippard[1] lists essentially all the mechanistic variants currently under consideration.

This survey of the experimental results shows that a large number of important issues in the chemistry of MMO remain to be resolved. Only recently has it become possible to attempt systems of the complexity of MMO by advanced theoretical methods. During the past decade there has been very rapid progress in the application of such methods to transition metals, both in the area of conventional *ab initio* methods but even more so in the area of Density Functional Theory (DFT).[17−19] Only a few years ago, a computation even on a small complex containing a transition metal was considered a major project with many uncertainties. More recently, accurate calculations on realistic transition metal complexes have become possible and an increasing number of such studies have been performed, see for example refs 20 and 21. In spite of this progress, no attempt has so far been made to treat a system with a complexity approaching that of the diiron site in MMO. The difficulties are manyfold. The spin on the metal atoms is unusually high leading to the presence of many open-shell electrons. For example, for the oxo structure of the present diiron complex the ground state with ferromagnetic coupling of the metal spins is ^{11}A. Previously, mostly closed shell systems have been treated. Furthermore, very few complexes containing two transition metal atoms have so far been treated and first-row transition metal complexes are generally considered much more difficult to treat computationally than second or third-row complexes. In addition, the system treated is quite large. The present study is also concerned with a reaction, which means that apart from stationary points, transition states are also of interest; these are considerably harder to locate. Finally, the lack of experimental information on the enzyme as precise as is possible for small molecule systems is, of course, an additional complication. Nevertheless, the present study is performed with few compromises in the theoretical treatment. The DFT method chosen, the B3LYP method,[22] is the one which has been proven by benchmark test calculations to be the most reliable available. It contains Hartree−Fock exchange, a mixture of exchange and correlation functionals including gradient corrections of the density, and carefully chosen empirical parameters obtained from fitting to accurate experiments. Also, the basis sets used in the present study would be considered very large even if for a small system with light atoms. All degrees of freedom have been optimized for all structures. Furthermore, for the most important points, Hessians have been evaluated, requiring more than 200 h of computation time per point.

The quantum chemical work described in this paper, while

(7) Ortiz de Montellano, P. R. *Cytochrome-P-450*; Plenum Press: New York, 1985.
(8) Andersson, K. K.; Froland, A.; Lee, S.-K.; Lipscomb, J. D. *New J. Chem.* **1991**, *15*, 411.
(9) Jiang, Y.; Wilkins, P. C.; Dalton, H. *Biochim. Biophys. Acta* **1993**, *105*, 1163.
(10) Proniewicz, L. M.; Bajdor, K.; Nakamoto, K. *J. Phys. Chem.* **1986**, *90*, 1760.
(11) Stassinopoulos, A.; Caradonna, J. *J. Am. Chem. Soc.* **1990**, *112*, 7071.
(12) Leising, R. A.; Brennan, B. A.; Que, L., Jr. *J. Am. Chem. Soc.* **1991**, *113*, 3988.
(13) Ruzicka, F.; Huang, D. S.; Donnelly, M. I.; Frey, P. A. *Biochemistry* **1990**, *29*, 1696.
(14) Priestley, N. D.; Floss, H. G.; Froland, W. A.; Lipscomb, J. D.; Williams, P. G.; Morimoto, H. *J. Am. Chem. Soc.* **1992**, *114*, 7561.
(15) Liu, K. E.; Johnson, C. C.; Newcomb, M.; Lippard, S. J. *J. Am. Chem. Soc.* **1993**, *115*, 939.
(16) Leising, R.; Brennan, B. A.; Que, L.; Fox, B. G.; Munck, E. *J. Am. Chem. Soc.* **1991**, *113*, 3988.
(17) Siegbahn, P. E. M. *Adv. Chem. Phys.* **1996**, *93*, 333.
(18) Ziegler, T. *Chem. Rev.* **1991**, *91*, 651.
(19) Salahub, D. R.; Castro, M.; Fournier, R.; Calaminici, P.; Godbout, N.; Goursot, A.; Jamorski, C.; Kobayashi, H.; Martinez, A.; Papai, I.; Proynov, E.; Russo, N.; Sirois, S.; Ushio, J.; and Vela, A. In *Theoretical and Computational Approaches to Interface Phenomena*; Sellers, H., Olab, J., Eds.; Plenum: New York, 1995; p 187.
(20) Lohrenz, J. C. W.; Woo, T. K.; Ziegler, T. *J. Am. Chem. Soc.* **1995**, *117*, 12793.
(21) Siegbahn, P. E. M. *J. Phys. Chem.* **1996**, *100*, 14672.
(22) Becke, A. D. *Phys. Rev.* **1988**, *A38*, 3098. Becke, A. D. *J. Chem. Phys.* **1993**, *98*, 1372. Becke, A. D. *J. Chem. Phys.* **1993**, *98*, 5648.

only an initial step, nevertheless allows several useful proposals to be suggested about the relationship between the enzyme structure and its function. First, the structures of several different proposed model intermediates were found. These include, the Fe_2(IV,IV) bis-μ-oxo intermediate, the Fe_2(III,III) peroxo intermediate, the Fe_2(II,III) superoxo intermediate, and the Fe_2(III,IV) oxo intermediate. The ligands were chosen to be as simple as possible: hydroxyl and water groups. Five- and six-coordination were investigated and the role of Jahn−Teller distortion in helping to generate the reactive iron oxo species. The reaction with methane was then approached by studying several possible reaction products. Finally, the transition state for the most interesting pathway was determined. Many of the results obtained are in reasonable agreement with what is known experimentally for MMO. More importantly, new results are obtained leading to suggestions of a possible intermediacy of a species with an Fe−CH_3 bond.

II. Computational Details

The calculations were performed in two steps. First, an optimization of the geometry was performed using B3LYP, a Density Functional Theory (DFT) type of calculation based on hybrid functionals, and double-ζ basis sets. In the second step the energy was evaluated in the optimized geometry using very large basis sets including diffuse functions and with two polarization functions on each atom. The final energy evaluation was also performed at the B3LYP level. All calculations were performed using the GAUSSIAN-94 program.[23]

The present DFT calculations were made using the empirically parametrized B3LYP method.[22] The B3LYP functional can be written as,

$$F^{\mathrm{B3LYP}} = (1-A)F_x^{\mathrm{Slater}} + AF_x^{\mathrm{HF}} + BF_x^{\mathrm{Becke}} + CF_c^{\mathrm{LYP}} + (1-C)F_c^{\mathrm{VWN}}$$

where F_x^{Slater} is the Slater exchange, F_x^{HF} is the Hartree−Fock exchange, F_x^{Becke} is the gradient part of the exchange functional of Becke,[22] F_c^{LYP} is the correlation functional of Lee, Yang, and Parr,[24] and F_c^{VWN} is the correlation functional of Vosko, Wilk, and Nusair.[25] *A*, *B*, and *C* are the coefficients determined by Becke[22] using a fit to experimental heats of formation. However, it should be noted that Becke did not use F_c^{VWN} and F_c^{LYP} in the expression above when the coefficients were determined, but rather the correlation functionals of Perdew and Wang.[26]

The B3LYP energy calculations were made using the large 6-311+G(2d,2p) basis sets in the Gaussian-94 program. This basis set has two sets of polarization functions on all atoms, and also diffuse functions which are found to be important when interactions with oxygen-containing systems like water are studied. This basis set will be referred to as the large basis set. In the B3LYP geometry optimizations a much smaller basis set, the LANL2DZ set of the Gaussian-94 program, was used. For the iron atom this means that a non-relativistic ECP according to Hay and Wadt[27] was used. The valence basis set used in connection with this ECP is essentially of double-ζ quality including a diffuse 3d function. The rest of the atoms are described by standard double-ζ basis sets. This basis set will be referred to as the small basis set. In some of the points of main interest, Hessians were also calculated at essentially the same B3LYP level as the geometries were determined. An all-electron basis[28] was used on iron in order to allow analytic evaluation of the Hessians. For the equilibrium geometries determined there were no imaginary frequencies, and for the C−H activation transition states one imaginary frequency was found as required for a true transition state. Since the calculation of Hessians is very time consuming, over 200 h on a workstation, zero-point vibrational effects for some of the less important systems had to be estimated based on Hessian calculations for similar structures. All energies reported below and in the tables include zero-point vibration. Temperature effects will be only briefly discussed.

In many of the structures discussed below there are hydrogen bonds and a few comments can be made concerning the accuracy of these at the B3LYP level. First, very large basis sets as the ones used here are needed to obtain reliable hydrogen bond energies. In particular, diffuse functions and at least two sets of polarization functions are needed to get the dipole moment and polarizability of water correctly. The water dimer binding energy using the 6-311+G(2d,2p) basis set and including zero-point vibrational effects is 2.8 kcal/mol compared to the experimental value of 3.6 ± 0.5 kcal/mol, which must be considered a highly satisfactory result. Secondly, the hydrogen bond distances are somewhat too short at the present level of geometry optimization using only a medium size basis set, but the effect on the energies from the errors on the geometries is quite small. In a study such as this one where there are large uncertainties even on the actual ligands appearing in the second coordination shell, a higher level geometry optimization to obtain better hydrogen bond geometries does not seem meaningful.

III. Results and Discussion

The discussion of the results is divided into three subsections. In the first, the tests made for deciding on a proper chemical model for the present study are described. These tests include studies of iron monomer complexes with different oxidation states, different ligands, and different coordinations. The final choice of model for the bis-μ-oxo diiron complex is $Fe(OH)_2(H_2O)-O_2-Fe(OH)(H_2O)(OCHO)$. As a natural first step in a study of this type, the ligands were chosen as simple as possible. More realistic ligands can then be used in future studies to monitor any differences from the present results. A key feature of the model complex is the bridging carboxylate ligand, also present in the real system. In the second subsection, different isomers of the oxidized model are compared, starting with the bis-μ-oxo Fe_2(IV,IV) complex, and continuing with the peroxo, the superoxo, and oxo isomer complexes. The reaction with methane is discussed in the third subsection where also comparisons are made to the methane reaction with an iron−porphyrin model. It should be emphasized that due to the model character of the present approach, we can only delineate a plausible set of intermediates having facile interconversions, but cannot exclude other pathways that have not yet been tested.

a. The Chemical Model. A large part of the initial effort of the present project was spent in selecting a proper chemical model for the active iron dimer site of MMO for further study. Three different oxidation states of iron are involved in the iron dimer complexes, Fe(II), Fe(III), and Fe(IV). Of these the latter two turn out to be most important to model properly. The first investigation performed was a study of 6-coordinate iron monomer complexes with these three oxidation states. The simplest possible ligands were chosen, hydroxyl and water in most cases. The results were quite surprising. As shown in Table 1, it turns out that 5-coordination is highly competitive with 6-coordination for these systems, at least in the gas phase. It should be emphasized that the dielectric constant of an enzyme is not very high ($\epsilon \approx 4$) and is thus closer to the gas-phase value than the value in water ($\epsilon \approx 80$), for example.

The first systems studied were the Fe(IV) complexes $Fe(OH)_4(H_2O)_2$, where the high-spin ^{5}A state is the ground state. For

(23) GAUSSIAN 94 (Revision A.1), Frisch, M. J.; Trucks, G. W.; Schlegel, H. B.; Gill, P. M. W.; Johnson, B. G.; Robb, M. A.; Cheeseman, J. R.; Keith, T. A.; Petersson, G. A.; Montgomery, J. A.; Raghavachari, K.; Al-Lahm, M. A.; Zakrzewski, V. G.; Ortiz, J. V.; Foresman, J. B.; Cioslowski, J.; Stefanov, B. R.; Nanayakkara, A.; Challacombe, M.; Peng, C. Y.; Ayala, P. Y.; Chen, W.; Wong, M. W.; Andres, J. L.; Replogle, E. S.; Gomperts, R.; Martin, R. L.; Fox, D. J.; Binkely, J. S.; Defrees, D. J.; Baker, J.; Stewart, J. P.; Head-Gordon, M.; Gonzales, C.; Pople, J. A. Gaussian, Inc.: Pittsburgh, PA, 1995.

(24) Lee, C.; Yang, W.; Parr, R. G. *Phys. Rev.* **1988**, *B37*, 785.

(25) Vosko, S. H.; Wilk, L.; Nusair, M. *Can. J. Phys.* **1980**, *58*, 1200.

(26) Perdew, J. P.; Wang, Y. *Phys. Rev. B* **1992**, *45*, 13244. Perdew, J. P. In *Electronic Structure of Solids*; Ziesche, P.; Eischrig, H. Eds.; Akademie Verlag: Berlin, 1991. Perdew, J. P.; Chevary, J. A.; Vosko, S. H.; Jackson, K. A.; Pederson, M. R.; Singh, D. J.; Fiolhais, C. *Phys. Rev. B* **1992**, *46*, 6671.

(27) Hay, P. J.; Wadt, W. R. *J. Chem. Phys.* **1988**, *82*, 299.

(28) Wachters, A. J. H. *J. Chem. Phys.* **1970**, *52*, 1033.

Table 1. Relative Energies (kcal/mol) for Some 5- and 6-Coordinate Fe(III) and Fe(IV) Monomer Complexes[a]

complex	state	oxidation state	coord no.	rel energy
$Fe(H_2O)_6^{2+}$	^5A	II	5	+8.1
			6	0.0
$Fe(OH)_3(H_2O)_3$	^6A	III	5	−8.0
			6	0.0
$Fe(H_2O)_6^{3+}$	^6A	III	5	+10.1
			6	0.0
$Fe(OH)_4(H_2O)_2$	^5A	IV	5	+1.1
			6	0.0
$Fe(OH)_4(NH_3)_2$	^5A	IV	5	+2.1
			6	0.0
$Fe(OH)_4(NHCH_2)_2$	^5A	IV	5	+1.9
			6	0.0

[a] The 5-coordinate complexes have one ligand in the second coordination shell. The relative energy is set to zero for the 6-coordinate complexes, and negative energies for the 5-coordinate complexes mean higher stabilities for these.

the small basis set used in the geometry optimization a 5-coordinate geometry with one water ligand hydrogen bonded in the second coordination shell, $[Fe(OH)_4(H_2O)](H_2O)$, is preferred by almost 5 kcal/mol. For the large basis set the preference is reversed with 6-coordination slightly preferred by 1.1 kcal/mol. This result is not particular for water ligands, but is essentially the same also for ammonia and imine ligands, see Table 1. The conclusion is that 5- or 6-coordinate complexes could be used equally well for modeling Fe(IV) oxidation states of the MMO complex. The only difference would be that if an empty site was required, for a 6-coordinate model a small energy (of the order of at most a few kilocalories per mole) would be required to open up this site. To be more explicit, if the real complex prefers 6-coordination over 5-coordination by 2 kcal/mol, and a calculation using a 5-coordinate model gives a barrier of 9 kcal/mol for the C−H activation of methane, then a good estimate of the barrier for the 6-coordinate case would be 9 + 2 = 11 kcal/mol. The difference between 9 and 11 kcal/mol can be considered to fall within the errors bars of the present modeling. The dynamics of the methane reaction would be modified if there were a barrier between the 5- and 6-coordinate complexes, but the effect would not be large if this barrier is substantially smaller than the one for C−H activation. It must be added that since the experimentally determined structure, see Figure 1, has 6-coordinate iron centers, future studies should obviously investigate also such structures. That type of study would probably also need to take into account outer-sphere interactions and require other ligands than hydroxyl and water. The conclusion reached here based on the present model calculations is simply that we do not expect a choice of model where 6-coordination is slightly preferred to seriously affect the main conclusions of the present study. Another conclusion that can be drawn from the results in Table 1 is that it is not critical for the coordination if oxygen-based or nitrogen-based ligands are used. This conclusion is also true concerning the spin and charge distribution. Since the actual MMO complex, see Figure 1, has one nitrogen-based ligand on each iron center it could be argued that the present model also should have one such ligand, but the results in Table 1 show that this is unlikely to change any of the qualitative results reached here. A major reason for the decision to use only oxygen-based ligands was that this should simplify comparisons to similar calculations done simultaneously on manganese dimer complexes, where only oxygen-based ligands were used. To some extent, the use of one type of ligand also simplifies the conclusions from the present study.

The low-spin ^3A state of the $Fe(OH)_4(H_2O)_2$ complex was found to be 11.8 kcal/mol higher in energy than the ^5A state. For the ^5A state the 6-coordinate isomer with the two water ligands trans to each other was found to be more stable than the cis species by as much as 32.5 kcal/mol. The trans preference can be easily explained by ligand field theory. For these octahedral Fe(IV) complexes there is only one repulsive e-electron, which can only be avoided by the strongly bound hydroxyl ligands if they are all in one plane, leading to the trans structure.

Table 2. Metal Charge, Spin, and 3d Population for Some Iron Monomer Complexes with Different Oxidation States and Coordinate[a]

complex	state	oxidation state	coord no.	*Q*(Fe)	spin(Fe)	3d(Fe)
$Fe(OH)_2(H_2O)_4$	^5A	II	4	+0.96	3.75	6.31
$Fe(H_2O)_6^{2+}$	^5A	II	5	+1.11	3.81	6.26
			6	+1.04	3.84	6.26
$Fe(OH)_3(H_2O)_3$	^6A	III	5	+1.01	4.02	6.09
			6	+0.82	4.08	6.10
$Fe(H_2O)_6^{3+}$	^6A	III	5	+1.45	4.21	5.93
			6	+1.11	4.25	5.94
$Fe(OH)_4(H_2O)_2$	^5A	IV	5	+0.85	3.20	6.27
			6	+0.61	3.26	6.28

[a] The 5-coordinate complexes have one ligand in the second coordination shell.

For the Fe(III) complex $Fe(OH)_3(H_2O)_3$, 5-coordination is even more favorable than for the Fe(IV) complexes discussed above. For the high-spin ^6A ground state of this complex, 5-coordination is actually preferred by 8.0 kcal/mol over 6-coordination using the large basis set. The excitation energy to the low-spin state ^4A is 13.2 kcal/mol, which is about the same as the corresponding excitation energy for the Fe(IV) complex. For the Fe(II) complex $Fe(OH)_2(H_2O)_4$, the geometry actually converged to a 4-coordinate isomer with the water ligands in the second shell. No particular effort was spent to try to converge this complex to 5- or 6-coordination since Fe(II) complexes play a very minor role in the present study. The ground state of the Fe(II) complex is also high-spin, ^5A, with an excitation energy to the low-spin ^3A state of 24.5 kcal/mol, somewhat higher than for Fe(III) and Fe(IV). In summary, with the present choice of ligands, Fe(III) complexes and probably also Fe(II) complexes are best modeled as 5-coordinate.

Since the preference for 5-coordination is in contradiction with experimental data for iron salts dissolved in water,[29] a few additional complexes with only water ligands were investigated. In line with experimental results, both $Fe(H_2O)_6^{2+}$ and $Fe(H_2O)_6^{3+}$ were found to strongly prefer 6-coordination, by 8.1 and 10.1 kcal/mol, respectively. There is thus no conflict between experimental water solution results and the present calculations. The conclusion is instead that an $Fe(H_2O)_6^{n+}$ ion is quite different from an $Fe(OH)_n(H_2O)_{6-n}$ complex, even though they have the same oxidation states. A neutral complex should be a much better representation of the diiron complex in MMO since the dielectric constant is so low. It can be added that for $Fe(H_2O)_6^{4+}$ no reasonable geometry could be obtained. Instead, dissociation of a H_2O^+ ligand was found.

For the later analysis of the more complicated dimer complexes, some results of the population analyses of the monomer complexes are gathered in Table 2. It should be remembered that charges obtained from the Mulliken population analysis have large uncertainties, in particular for the charges related to diffuse functions. For this reason, the iron 4s and 4p populations are not discussed. The uncertainty of the total charge on iron can be estimated to be ±0.3 since this is the difference of the charges going from the smallest to the largest basis set. From a normal chemical point of view, the populations in Table 2 are quite surprising. For example, the charge

(29) Hasker, P. N.; Twigg, M. V. In *Encyclopedia of Inorganic Chemistry*; King, R. B., Ed.; Wiley: New York, 1994; Vol. 4, p 1698.

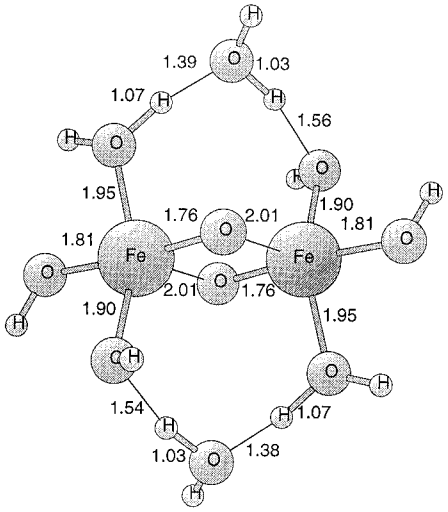

Figure 2. The result of the geometry optimization for the ^{9}A state of $Fe(OH)_2(H_2O)_2-(\mu\text{-}O)_2-Fe(OH)_2(H_2O)_2$. The starting geometry for the optimization was two octahedrally 6-coordinate iron atoms linked by μ-oxo bridges. The distance between the bridging oxygens is 2.51 Å.

on iron is much smaller than expected from a literal interpretation of the oxidation state and does not even increase with the oxidation state. For the Fe(II) complex it is +0.96, for the Fe(III) complex +1.01 (5-c) or +0.82 (6-c), and for Fe(IV) complex +0.85 (5-c) or +0.61 (6-c). The 3d population is quite stable slightly above 6. This is the same number of 3d electrons as in the ground state (d^6s^2) of the free neutral iron atom and indicates that it is energetically costly to significantly change this 3d population. The property that is most sensitive to the oxidation state is the spin on iron. In line with the higher spin of the ground state for the Fe(III) complexes, ^{6}A, the spin on iron is highest, around 4.0, for this oxidation state. Fe(II) has slightly lower spin of 3.75, while Fe(IV) has the lowest spin of about 3.2. Overall, roughly one unit of spin is delocalized over the ligands for all oxidation states. This is quite different from the corresponding manganese complexes.[30] This difference can therefore be identified as an important factor which leads to distinct differences in the chemistry of manganese and iron complexes. The spin population on the metal is the best measure of the oxidation state of the iron atoms in the dimer and will be used in the analysis of these complexes below. Even though part of the difference between the numbers in Table 2 and the conventional chemical picture of the charges and 3d populations of these complexes results from the arbitrariness of the Mulliken population analysis, as mentioned above, most of it is certainly due to the oversimplified form of the conventional chemical picture.

Model complexes used for the iron dimer in compound **Q** of MMO were diiron(IV) bis-μ-oxo complexes. To allow for both 5- and 6-coordination of the iron atoms the Fe_2(IV,IV) complex used was $Fe(OH)_2(H_2O)_2-(\mu\text{-}O)_2-Fe(OH)_2(H_2O)_2$. The starting geometry had two octahedral 6-coordinate iron atoms. The outcome of the geometry optimization for this complex is shown in Figure 2.

At first sight, the structure shown in Figure 2 is very abnormal: the Fe(IV) is 5-coordinate rather than the expected 6-coordinate and the two oxo groups are asymmetrically placed between the Fe atoms so that the two M−O (oxo) bond lengths for each metal are substantially unequal. While we lack crystal structures for relevant Fe(IV) systems of this type, which are insufficiently stable for X-ray crystallographic or other structural study, many bis-μ-oxo dimanganese(III,IV) dimers are structurally characterized[30] and these provide a starting point for a comparison with the Fe(IV) case because Mn(III) is also a d^4 ion. In these clusters, the Mn(III) center is generally octahedral, but the ligands are usually chelating or at least more strongly binding than the OH_2 of the computational model system. Again in the Mn dimers, the Mn(III) center shows strong Jahn−Teller (JT) distortions, as expected for a d^4-octahedral high-spin ion, with two long and four short M−L distances, but the bis-μ-oxo ligands are always involved in the short M−L distances and the two Mn−O(oxo) distances are therefore substantially equal. The long M−L distances arising from the Jahn−Teller distortion are found in the ligands perpendicular to the $Mn-(\mu\text{-}O)_2-Mn$ plane. This pattern appears both in the experimental structures and in DFT calculations on Mn oxo clusters carried out by the same methods used in this paper.[31]

In the Fe_2(IV,IV) species of Figure 2, we regard the observed structure as being derived from an octahedron, but showing strong Jahn−Teller (JT) distortions. The JT axis, along which the M−L bonds are elongated, is not the axis normal to the $M-(\mu\text{-}O)_2-M$ plane, as in the Mn(III) case, but is the axis defined by the long M−oxo bond and the vacant site trans to it; this vacancy we interpret as an extreme case of JT distortion leading to the departure of the OH_2 ligand, assisted by the relatively strong second sphere hydrogen bonding that it can engage in when no longer bound to iron. We also find the expected four short M−L bonds in the plane normal to the JT axis. Of these four short bonds, one is formed to a water molecule, two to hydroxo, and one to bridging oxo. The quantum chemical studies indicate that only the structure shown in Figure 2 has any significant stability—no other Jahn−Teller distortional isomers were found.

A second way to view the structure of the diiron cluster is that the JT axis along which M−L bonds are elongated is automatically defined by the position of the ligand lost from the cluster. In this way the enzyme can control the orientation of the JT axis, because bound water may be lost easily, but the ligating groups derived from the polypeptide are much less likely to be lost. The bridges present both in the present model in Figure 2 and in the actual complex in Figure 1 force the ligand lost to be in the $Fe-(\mu\text{-}O)_2-Fe$ plane and therefore also the JT axis to be in this plane. This causes the large asymmetry in the bridging Fe−oxo distances, which, as we will see in detail below, in turn allows the less reactive bridging oxo to open up to a terminal oxo, alone capable of reacting rapidly with methane. This aspect of the structure/function relationship could not have been postulated from a knowledge of the behavior of other d^4 ions such as Mn(III) but in the absence of structural data, can only come from quantum chemical studies.

In order to test the interpretation of the structures based on JT distortions made above, a few additional calculations were performed. First, the bridging waters in the structure in Figure 2 were removed. The remaining ligands were then placed in such a way that the more weakly bound water ligands and the empty sites were located perpendicular to the $Fe-(\mu-O)_2-Fe$ plane, which should force the JT axis also to be perpendicular to this plane, if the analysis is right. The optimized geometry for this structure is in full agreement with this analysis leading to four equal Fe−O μ-oxo bonds. As a second test of the JT analysis, the iron atoms in Figure 3 were replaced by manganese atoms and the two hydroxyl ligands trans to the Mn−O μ-oxo bonds were replaced by water ligands. This should force the JT axis of this Mn_2(III,III) complex to fall in the $Mn-(\mu\text{-}O)_2-$

(30) Manchanda, R.; Brudvig, G. W.; Crabtree, R. H. *Coord. Chem. Rev.* **1995**, *144*, 1.

(31) Blomberg, M. R. A.; Siegbahn, P. E. M.; Styring, S.; Babcock, G. T.; Åkermark, B.; Korall, P. Submitted for publication.

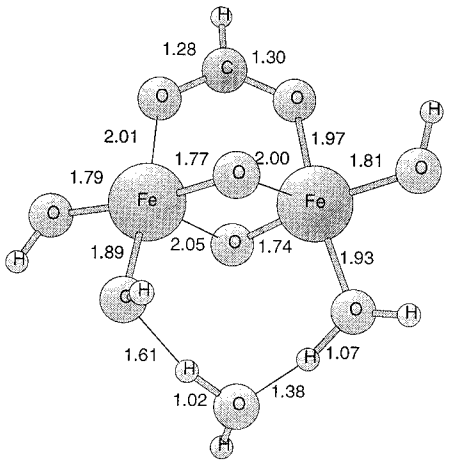

Figure 3. The optimized ^{9}A $Fe^{IV}-(\mu\text{-}O)_2-Fe^{IV}$ structure. The computed energy for this structure relative to the lowest O_2 structure, the one in Figure 4, is +5.2 kcal/mol. The distance between the bridging oxygens is 2.56 Å.

Mn plane. In line with this reasoning, the Mn−O μ-oxo bonds are now unequal, just as in the Fe_2(IV,IV) structures in Figures 2 and 3.

A few additional comments can be made on the structure in Figure 2. As already mentioned, both in this complex and in the real MMO complex there are bridges between the iron atoms in addition to the oxo bridges; in the real complex the bridges are formed by glutamate ligands while in the model system hydroxyl and water form the bridges. In order to gain authenticity, one of the water bridges was therefore replaced by formate which is used as a model for glutamate. There is an interesting parallel between the glutamate bridge and the water bridge. Glutamate has two coordinating oxygens. In formal terms, one of them will form a covalent bond to one iron atom and the other a coordination bond to the second iron atom (or both bonds will be a mixture of these types). This means that glutamate has the ability to easily shift the oxidation states of the iron atoms. In a similar way, the water bridges can change the oxidation states by hydrogen atom transfer in the chain. This effect was actually noticed in several cases during the geometry optimization; the water bridge changed from Fe···(H_2O)···(H_2O)···(OH)−Fe to Fe−(OH)···(H_2O)···(H_2O)···Fe. In this hydrogen transfer reaction, the leftmost iron atom increases its oxidation state by +1 while the oxidation state for the rightmost iron atom is changed by −1. The same effect is achieved when Fe←(OCHO)−Fe is changed to Fe−(OCHO)→Fe.

In what follows, $Fe(OH)_2(H_2O)-(\mu\text{-}O)_2-Fe(OH)(H_2O)$-(OCHO) models will thus be used for the active site of MMO. There is one additional important model assumption made and this concerns the spin. In the real systems, the spins on the iron atoms in the oxidized core are thought to be antiferromagnetically coupled. This conclusion is based on magnetic, EPR, and model studies.[32] Antiferromagnetic coupling is extremely difficult to handle in the present type of calculations, partly because convergence to the correct state is seldom achieved. Nor is low-spin coupling strictly correctly handled in a DFT approach such as B3LYP. Therefore, it would be computationally much preferable if the present systems could be modeled with a ferromagnetic coupling. In a recent study of a similar manganese dimer complex in PSII,[31] the assumption of ferromagnetic coupling was tested. In that case convergence was actually achieved for both spin couplings for a few systems, and ferromagnetic and antiferromagnetic coupling lead to very similar energies and almost identical structures. It can be noted as an additional point of interest that antiferromagnetic coupling was actually preferred by the B3LYP method by a small, but quite reasonable amount of energy (about 2 kcal/mol) even though spin is not correctly handled with this method. It appears that as long as there is small overlap between the metal orbitals the energy expression used in B3LYP will still work reasonably well. Ferromagnetic coupling of the iron spins was therefore used throughout in the present study.

b. Relative Stabilities of Fe−O_2−Fe Structures. The first $Fe(OH)_2(H_2O)-O_2-Fe(OH)(H_2O)$(OCHO) structure that will be discussed here is the $Fe^{IV}-(\mu\text{-}O)_2-Fe^{IV}$ structure, since it shows characteristic features of Fe(IV) chemistry that reappear throughout the study. Experimental data are readily available for Fe(II) and Fe(III), but there are so few Fe(IV) species known that theory is a prime method to learn about the chemistry of this oxidation state. The result of the geometry optimization is shown in Figure 3. It can first be noted that the structure is extremely similar to the one for $Fe(OH)_2(H_2O)_2-(\mu\text{-}O)_2-Fe$-$(OH)_2(H_2O)_2$ shown in Figure 2. The central part of the molecule is virtually identical in the two models, and suggest that the chemistry are likely to be the same. This is one indication that qualitative results obtained in the present model calculations should be broadly independent of the exact choice of ligands. As already discussed, the bis-μ-oxo bridge has the rather surprising feature that the Fe−O bonds are not all the same length with two short bonds, 1.74 and 1.77 Å, and two long bonds, 2.00 and 2.05 Å. The most reasonable bonding picture gives the shorter bonds partial double bond character and the longer bonds partial coordinate bonding character. The ground state of this complex with ferromagnetic coupling is ^{9}A and the spin on each iron atom, 3.03 and 3.14 (see Table 2), is quite characteristic of the Fe(IV) oxidation state. There is thus no tendency for mixing in Fe(III) character. The bridging oxygen atoms have a large degree of radical character with spin populations of 0.60 and 0.69, respectively, which is a large part of the explanation for the particular reactivity of these systems. Another indication of the high reactivity is the low adiabatic excitation of 4.3 kcal/mol to the ^{11}A state (computed using the small basis set for the model in Figure 2). This means that the highly reactive oxo species is easily accessible, see further below.

Three additional comments on the structure in Figure 3 will be made. First, the bridging formate group has more covalent character in one of its Fe−O bonds, which is necessary to balance the oxidation states of the iron atoms since the other iron atom has one more hydroxyl ligand. Second, the hydroxyl groups on the backside of the iron atoms are trans to the short μ-oxo Fe−O bonds, which is surprising but is explained by the orientation of the JT axis in the $Fe-(\mu-O)_2-Fe$ plane forced by the presence of the bridging ligands. Third, there are some rather short O−H hydrogen bonds in the water bridge. Even if this effect is somewhat exaggerated by the small basis set, the short O−H distances indicate that the hydrogen atoms in these bridges are quite mobile. Indeed, for several model structures used in the present study, hydrogen atoms move from one oxygen atom to another during the geometry optimization.

The second structure optimized was the peroxo $Fe^{III}-(\mu\text{-}O_2)-Fe^{III}$ structure shown in Figure 4, expected to be formed from reaction of the MMO Fe_2(II,II) reduced state with O_2, and for which a model compound has been reported by Kim and Lippard.[33] The ground state is ^{11}A and it has iron spins of 3.94 and 3.97, typical of Fe(III), complexes (see Table 2). The molecular O−O distance of 1.50 Å is typical of an O−O single bond at this level, as expected. The optimized O−O distance

(32) Kurtz, D. M. In *Encyclopedia of Inorganic Chemistry*; King, R. B., Ed.; Wiley: New York, 1994; Vol. 4, p 1698.

(33) Kim, K.; Lippard, S. J. *J. Am. Chem. Soc.* **1996**, *118*, 4914.

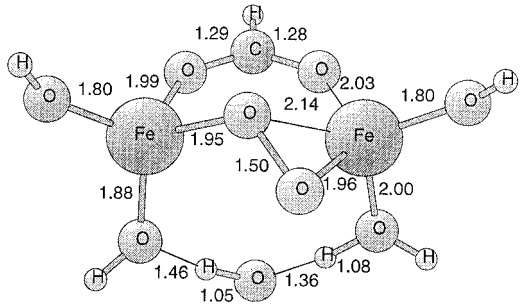

Figure 4. The optimized ^{11}A peroxo $Fe^{III}-(\mu\text{-}O_2)-Fe^{III}$ structure. This is the lowest energy O_2 structure of the present model system.

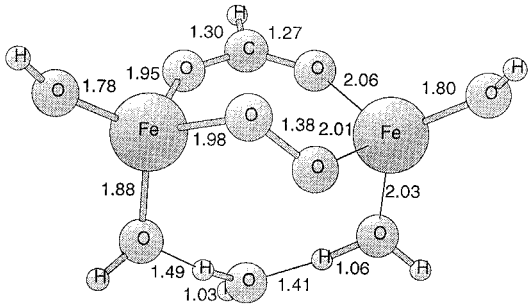

Figure 5. The optimized ^{9}A superoxo $Fe^{III}-(\mu\text{-}O_2)-Fe^{II}$ structure. The computed energy for this structure relative to the lowest O_2 structure, the one in Figure 4, is +12.9 kcal/mol.

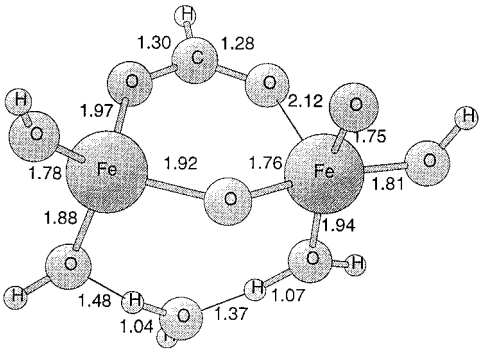

Figure 6. The optimized ^{11}A oxo formally $Fe^{III}-O-Fe^{V}=O$ structure. It is probably better regarded as $Fe^{III}-O-Fe^{IV}-O^{\bullet}$, however. The computed energy for this structure relative to the lowest O_2 structure, the one in Figure 4, is +4.5 kcal/mol.

in free H_2O_2 is 1.51 Å. However, the high spin population on O_2 in the peroxo species of 0.80 indicates a somewhat more complicated bonding pattern than the one in H_2O_2. The Fe−O bridge bonds of 1.96 and 1.95 Å are also typical single bonds. There is also an additional oxygen lone-pair bond of 2.14 Å to one of the iron atoms that distorts the geometry somewhat from a perfectly symmetric structure. Rather surprisingly, the peroxo species in Figure 4 is the lowest energy form of the present $Fe-O_2-Fe$ system and is 5.2 kcal/mol lower than the bis-μ-oxo structure in Figure 3. One major reason for the relatively low stability of the bis-μ-oxo structure is that the bridging ligands force the JT axis to be in the $Fe-(\mu\text{-}O)_2-Fe$ plane as discussed above. For the peroxo complex there is no such problem since it is a Fe_2(III,III) complex. It should also be pointed out that there is a clear tendency for increasing relative stability of the bis-μ-oxo structure with increasing basis set size. For the small basis set, the peroxo structure is favored by as much as 20.8 kcal/mol, which goes down to 7.8 kcal/mol for the 6−311+G(1d,1p) basis and to 5.2 kcal/mol for the largest basis set. A still larger basis set size could bring down the energy difference still further. Both the peroxo and the bis-μ-oxo structures have spins of the same size on the iron atoms, and antiferromagnetic coupling of these spins would thus lead to diamagnetic complexes. They are thus both candidates for compound **Q**, recently identified experimentally as a probable active intermediate in MMO.[5,16] In one experimental study on *M. trichosporium*,[16] the Mössbauer spectrum indicates two indistinguishable Fe(IV) atoms, supporting a bis-μ-oxo structure for compound **Q**. In another study on *Mc. capsulatus* (Bath)[5] the iron atoms were not found to be similar, thus it is more in line with the peroxo species, which has one more lone-pair bond to the peroxo ligand for one of the iron atoms. It is interesting to note that the peroxo and the bis-μ-oxo structures were recently found experimentally to have very similar energies for a dicopper model related to the copper oxidases and having a similar general structure.[34] In the copper case a change of solvent is enough to switch the most stable structure from one form to the other, which also means that the barrier between them is very small. It is expected that the barrier between the peroxo and bis-μ-oxo forms of the present complex should also be very small, but this has not yet been tested.

Another possible intermediate molecular oxygen species is the superoxo $Fe^{III}-(\mu\text{-}O_2)-Fe^{II}$ species shown in Figure 5. This species has a ^{9}A ground state with iron spins of 3.97 and 3.53. The spin on O_2 is 0.55, which is smaller than for the peroxo species in Figure 4 and directed in the opposite direction to the spins on the iron atoms. The energy for the superoxo complex in Figure 5 is 12.9 kcal/mol higher than that for the peroxo complex in Figure 4. It could play a role as an intermediate in oxygen capture by the initial Fe(II)−Fe(II) complex in the catalytic cycle. The O−O bond length of 1.38 Å is also in between those in free O_2 (1.21 Å) and the peroxo complex (1.50 Å).

The most significant $Fe-O_2-Fe$ structure discussed here is the formally Fe_2(III,V) Fe−O−Fe═O oxo structure shown in Figure 6 with only one bridging oxygen. The ground state of this structure is ^{11}A and the iron spins are 4.00 and 2.94, clearly showing a $Fe^{III}-O_2-Fe^{IV}$ structure (see Table 2). The spin on the bridging oxygen is 0.76 and on the oxo ligand it is as high as 1.13, showing that this species is better regarded as $Fe^{III}-O-Fe^{IV}-O^{\bullet}$, with an oxo group having radical character, and thus expected to be extremely reactive. The energy of the oxo complex is almost the same as for the bis-μ-oxo complex, and only 4.5 kcal/mol higher than for the peroxo complex. Also, the low-spin ^{9}A form of the oxo complex has a very similar energy. All three types of complexes, the bis-μ-oxo, the peroxo, and the oxo structures, are thus very close in energy, and it could be a question of the precise environment which of the systems is most stable. Second coordination effects could, for example, modify the stabilities as might changes in the ligands. As mentioned above, a still higher level of computational treatment may also lead to a higher relative stability of the bis-μ-oxo complex. At the present qualitative level, the conclusion is that these systems are of very similar energy and all of them will be easily accessible in the real MMO enzyme. Since $M-(\mu\text{-}O)_2-M$ ring opening to a M−O−M═O structure is not found[31] for Mn(III) where the bis-μ-oxo bridges are symmetrical, we propose that the asymmetric oxo bridges in the bis-μ-oxo structure of Figure 3, resulting from JT effects, facilitate this rearrangement.

c. The Methane Activation Reaction. The key experimental results from the introduction are first, the KIE of 4.2 is quite high indicating a hydrogen abstraction type reaction, but not as high as for P-450, where product radicals have actually been observed. Very fast radical clock measurements for MMO are also found to be inconsistent with the intermediacy of free

(34) Halfen, J. A.; Mahapatra, S.; Wilkinson, E. C.; Kaderli, S.; Young, V. G., Jr., Que, L., Jr.; Zuberbühler, A. D.; Tolman, W. T. *Science* **1996**, *271*, 1397.

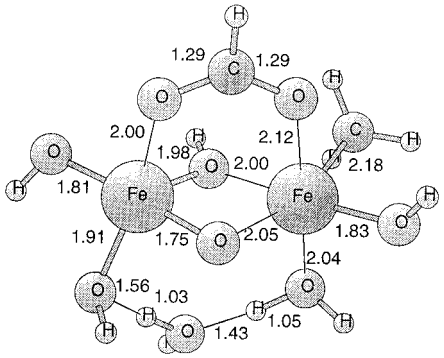

Figure 7. The low-spin ^{9}A C−H activated Fe_2(IV,III) product of the methane reaction with the abstracted hydrogen bound to a bridging oxygen. The computed energy for the reaction between methane and the lowest O_2 structure, the one in Figure 4, is +1.2 kcal/mol (endothermic).

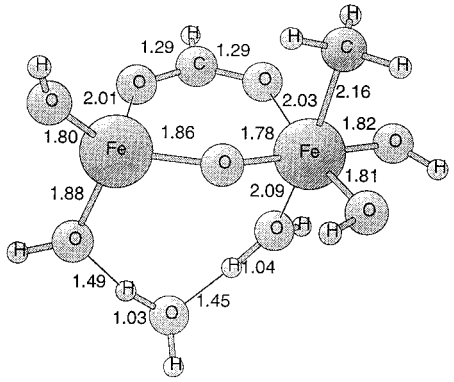

Figure 8. The low-spin ^{9}A C−H activated Fe_2(III,IV) product of the methane reaction with the abstracted hydrogen bound to a nonbridging oxygen. The computed energy for the reaction between methane and the lowest O_2 structure, the one in Figure 4, is −6.4 kcal/mol (exothermic).

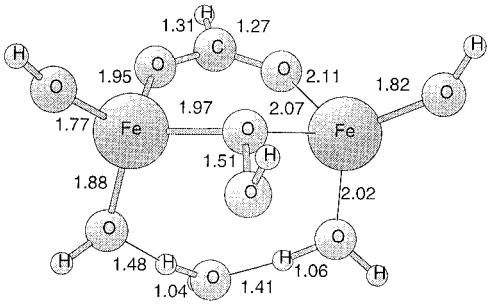

Figure 9. The structure of the ^{10}A Fe_2(III,II) peroxide structure obtained after hydrogen abstraction by the peroxo group of the Fe−(μ-O_2)−Fe structure in Figure 4. This peroxide structure is 35 kcal/mol less favorable than the corresponding structure in Figure 8 (without the methyl group).

radicals. Finally, for chiral ethane (CH_3CHDT) there is 35% inversion of configuration. Since in 65% of the reactions the configuration is retained, this result is also difficult to rationalize if truly free radicals have a more than transient existence.

In the study of the reaction between the different types of Fe−O_2−Fe complexes discussed above and methane, some possible products were first investigated. In the first type, the hydrogen abstracted from methane is bound to one of the bridging oxygens. This complex, without the remaining methyl group, was first studied by itself and found to have a ^{10}A ground state if ferromagnetic coupling is assumed, as above. Including the methyl group allows two possible spin states, a high-spin ^{11}A state or a low-spin ^{9}A state. The optimization of the high-spin state leads to the appearance of a free methyl radical. The optimization of the low-spin state leads to a rather surprising result with the methyl group directly bound to the iron atom, see Figure 7. The methyl group can be regarded as occupying the originally empty coordination site of a 5-coordinate bis-μ-oxo reactant, such as the one in Figure 3. The computated binding energy for the methyl radical, obtained by pulling the methyl group off and reoptimizing all degrees of freedom keeping the same position of the ligands, is quite small, 8.8 kcal/mol. The spins on iron for the structure in Figure 7 are 3.14 and 3.81, indicating a Fe_2(III,IV) complex. In line with this assignment, the spin is quite high (0.61) on the methyl group with a spin direction opposite to that for the iron atoms. By comparison of Figure 3, it can be seen that the bridging oxygen that has abstracted the hydrogen atom is the one with the short, 1.74 Å, distance to the iron atom that binds the methyl ligand. The alternative attack on the other iron atom in Figure 3 leads to an identical situation. For the direct reaction between methane and the bis-μ-oxo complex, there is thus only one possible reaction pathway if the methyl group ends up bound to an iron atom.

For the ^{10}A complex without the methyl group but with the hydrogen abstracted on a bridging oxygen, a few additional calculations were performed. It was then found that there is a rather big energetic advantage of 7.3 kcal/mol if the hydroxyl group on the backside of the iron atom avoids the trans position of the bridging hydroxyl group. Before the reaction, for the bis-μ-oxo complex in Figure 3, the backside hydroxyl group prefers to be trans to the short Fe−O bond, i.e. trans to the oxygen that abstracts the hydrogen from methane. This means that it would be ideal if the backside hydroxyl group would switch position during the methane attack, which is impossible (see Figure 7) if the methyl group should bind to the iron atom.

Since the methane attack on a briding oxygen of the bis-μ-oxo complex has the disadvantage described above, other product structures were investigated. Another possible attack could be on the oxo structure in Figure 6. In that case the product shown in Figure 8 is obtained. This approach has at least two advantages. First, the unfavorable trans orientation of the backside hydroxyl group with respect to a bridging hydroxyl group, discussed above, is avoided. Secondly, the oxo group of the structure in Figure 6 has substantial radical character (spin 1.13), which should be ideal for abstracting a hydrogen atom. Furthermore, the reacting oxo structure has about the same energy as the bis-μ-oxo structure. Indeed, the product in Figure 8 is 7.6 kcal/mol lower in energy than the product structure in Figure 7. With this gain in energy, the reaction between methane and the lowest energy Fe−(μ-O_2)−Fe isomer (the peroxo structure) is exothermic by 6.4 kcal/mol. The methyl group for the structure in Figure 8 is bound by 9.2 kcal/mol (using the small basis set), again obtained by pulling methyl off and reoptimizing the structure. The spins on iron in the product in Figure 8 are 3.99 and 2.94, leading to a Fe_2(III,IV) structure. It should be noted that this is opposite to that obtained by an attack on the bis-μ-oxo structure, where the product structure in Figure 7 is Fe_2(IV,III) instead. A structure was also optimized in which the methyl group and the hydroxyl group (with the abstracted hydrogen) in Figure 8 have switched positions. This leads to a structure with 2.5 kcal/mol higher energy, so it is less favorable.

A completely different type of product was also studied, obtained after hydrogen abstraction by the bridging peroxo group in Figure 4. This pathway is interesting mainly because the peroxo structure in Figure 4 was found to be the most stable Fe−O_2−Fe structure studied here. The resulting peroxide product structure, leaving out the methyl group, is shown in Figure 9. This turns out to be a surprisingly unfavorable structure. The energy is as much as 35 kcal/mol higher in

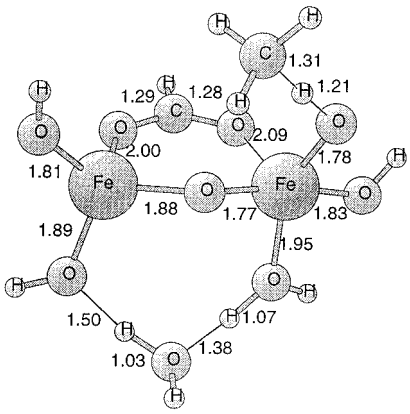

Figure 10. The structure of the ^{9}A transition state of the methane reaction. The computed barrier for the reaction between the lowest O_2 structure, the one in Figure 4, and free methane is +6.3 kcal/mol.

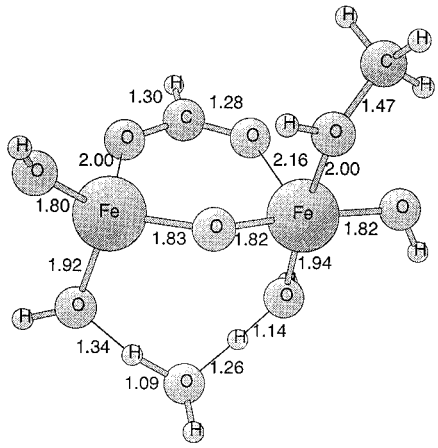

Figure 11. The low-spin ^{9}A Fe_2(III,III) methanol product of the methane reaction. The computed energy for the reaction between methane and the lowest O_2 structure, the one in Figure 4, is −40.3 kcal/mol (exothermic).

energy than the structure where a hydrogen has been abstracted by the oxo group in the structure in Figure 6. Therefore, methane attacks on bridging molecular oxygen structures can safely be ruled out. This result is in line with recent experiments.[35] The explanation for the poor energy of the peroxide structure is that the second oxygen loses all bonding to the iron atoms, which is clearly seen in the figure. The spins on the iron atoms are 4.01 and 3.71 leading to a Fe_2(III,II) structure.

The Fe_2(III,IV) structure in Figure 8 is thus the most favorable product structure after a methane attack. The reaction leading to this structure is exothermic by 6.4 kcal/mol with respect to free methane and the Fe−(μ-O_2)−Fe peroxo isomer. The first requirement on the reaction, that the reaction should be exothermic, is thus fulfilled. Starting with the structure in Figure 8 and moving the hydroxyl and methyl group closer together keeping constant distances to iron, a transition state optimization was made. This optimization finally led to the structure in Figure 10. The transition state identification of this structure was checked by computing a Hessian, which was found to have only one imaginary frequency as it should. The computed barrier height for activating methane, calculated with respect to the peroxo structure, is 6.3 kcal/mol. Based on earlier experience using the B3LYP method for similar hydrogen abstraction reactions, this value could be low by about 3 kcal/mol. In any event, the barrier height is low enough to indicate that this pathway is feasible for MMO. Zero-point vibration is found to have a large effect on the barrier, lowering it by 4.8 kcal/mol. This large effect is easily understood by inspection of Figure 10 where the almost pure hydrogen abstraction character can be noted. As a comparison, when a free methane molecule is divided into a free hydrogen atom and a free methyl radical, 9.7 kcal/mol zero-point vibration is lost.

With the identification of the transition state structure for the methane reaction, explanations for the main experimental results can be suggested. First, the large KIE for the reaction of 4.2 is clearly consistent with the type of transition state shown in Figure 10. As noted above, there is a large zero-point effect for the reaction barrier. For the same reason, there is also a large KIE. The calculated KIE for CD_4 at 298.15 K is 8.0, which is somewhat larger than the experimental value, indicating that the real transition state could be a little bit tighter with more bonding toward the metal. Quite recently, new experiments by Nesheim and Lipscomb[3b] have led to much larger KIE values for the methane reaction than the previous ones. For CD_2H_2 a value of 9 was found in close agreement with the calculated value. However, for CH_4:CD_4 an even larger value of 19 was measured. Large effects of tunneling were suggested to rationalize these large KIE values. Tunneling effects are not accounted for in the present simple estimate of the KIE value.

The second experimental result, 65% retention of configuration with chiral ethane, is in apparent contradiction with the formation of a nearly free methyl radical in the transition state of Figure 10. A reasonable explanation could be that after the transition state is passed, the Fe−CH_3 bond is very rapidly formed, leading to the product shown in Figure 8. If the transition state structure had a shorter Fe−C bond distance and the product had a stronger Fe−C bond (it is only 9.2 kcal/mol), 100% retention of configuration would be expected. Sixty five percent retention of configuration therefore appears reasonable and consistent with both the transition state and product structures found here. An explicitly calculated percentage retention would require a full dynamical treatment, as yet impossible, and stretch the qualitative model too far.

The final structure on the methane reaction pathway, the low-spin ^{9}A methanol product shown in Figure 11, is quite exothermic by 40.3 kcal/mol with respect to the peroxo structure. The low-spin structure was chosen since it is on the same spin surface as the methane product in Figure 8. The spins on iron are 3.98 and 2.76, indicating a low-spin Fe_2(III,III) structure. After the methanol product is formed, the remaining reaction step in the catalytic cycle is to form water from the oxygen in the bridge between the iron atoms. One possibility, an initial hydrogen abstraction from a nearby amino acid, make the O−H bond energy of a bridging hydroxyl group of some interest. The calculated value without the methanol product present is 72.7 kcal/mol. This can be compared to the O−H bond strength in tyrosine of 81.5 kcal/mol. This means that a direct abstraction from tyrosine is not possible using the present model system.

Finally, the transition state structure of Figure 10 was compared to a transition state structure obtained for a model of P-450, shown in Figure 12. The hydrogen abstraction character of each of the transition states is quite similar, and high KIE are thus expected in both cases, as was found experimentally. The calculated KIE for the P-450 model for CD_4 at 298.15 K is 10.2, which is well in line with the experimentally measured values that fall in the range 7−14. An important result, which is in agreement with experiments, is that the methane reaction is substantially endothermic for the P-450 model. The calculated endothermicity is 13.3 kcal/mol and the barrier is 22.7 kcal/mol. Experimentally only much weaker C−H bonds than the one in methane are activated by P-450. The large radical character of the oxo group in the structure in Figure 6 explains the better hydrogen abstraction ability of MMO. The easy

(35) Valentine, J. S.; Nam, W.; Ho, R. Y. N. *Act Dioxygen Homogeneous Catal. Oxid.* (*Proc. Int. Symp.*) *5th* **1993**, 183.

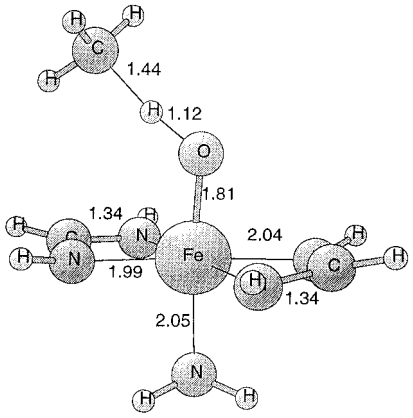

Figure 12. The $^3A''$ transition state structure (C_s symmetry) for the reaction between methane and the iron porphyrin model system. The barrier with respect to the $^3A''$ ground state of the reactant is 22.7 kcal/mol and the reaction energy to form the $^2A''$ hydrogen abstraction product is 13.3 kcal/mol (endothermic).

access to this oxo structure in MMO is explained by the presence of large JT distortions in the Fe−O_2−Fe plane.

The pathway described here helps reconcile some of the apparently inconsistent experimental data on MMO. The short alkyl radical lifetime indicated by radical clock probes seems inconsistent with the efficient trapping of methyl radical in *M. capsulatus* MMO reported by Dalton and coworkers using EPR spectroscopy and nitroxide spin traps.[36] The Fe^{III}−O−Fe^{V}-(CH_3)(OH) intermediate, proposed here, in which the methyl radical is bound to Fe by a weak Fe−C bond, helps reconcile these two sets of observations. The radical clock study, we propose, measures the very short lapse of time between the formation of the alkyl radical and its recombination with the iron center. The weak Fe−C bond of the Fe(V) methyl species allows this much longer lived species to be efficiently trapped by the nitroxide, at which point the methyl radical is transferred from Fe(V) to the nitroxide. On this model, the two observations refer to different processes and are therefore not inconsistent.

IV. Conclusions

We have tested a variety of plausible mechanisms for methane hydroxylation in MMO by high-level quantum chemical methods on model systems with simple ligands chosen on the basis of the MMO crystal structure and the available biophysical data. The sequence shown very schematically in Figure 13 gave acceptable energies for the intermediates and a low barrier for the CH abstraction step and therefore survives this first level of quantum chemical test. Although we cannot exclude its being eliminated in future studies, it at least provides a chemically and biochemically reasonable pathway. As pointed out by Feig and Lippard,[1] some of the experimental studies lead to conclusions that are not entirely in accord with each other, but our pathway is broadly in accord with the main experimental facts.

In this pathway, O_2 is assumed to add to the Fe_2(II,II) reduced form of MMO to give two peroxo species (**1** and **2**) and, after breaking the O−O bond, the bis-μ-oxo Fe(IV) dimer, **3**. An unexpected aspect of our findings includes the significant asymmetry of the oxo groups in this dimer (**3**), which was traced to the presence of large Jahn−Teller distortions of the d^4-iron centers as a result of the disposition in space of the active site ligands as revealed by the crystal structure. In this way the enzyme can control the orientation of the JT axis in the active site iron cluster and therefore its reactivity. It is proposed that

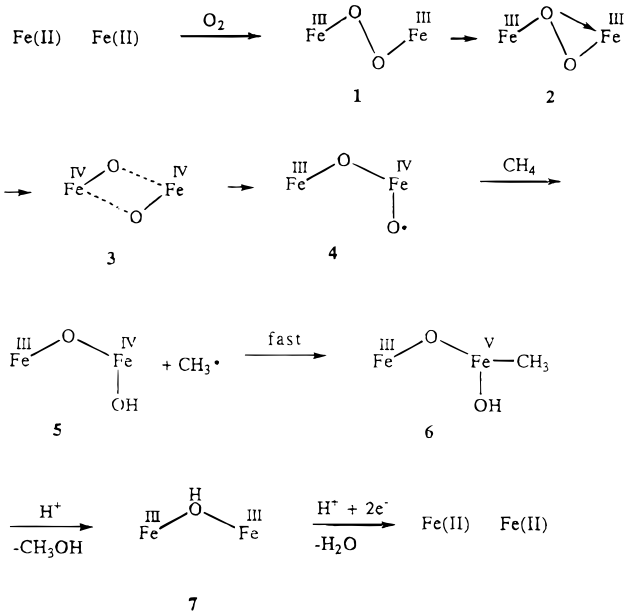

Figure 13. A schematic representation of the catalytic reaction sequence for the activation of methane by MMO leading to formation of methanol.

this asymmetry of the oxo groups in **3** facilitates its rearrangement to the key Fe^{III}−O−Fe^{V}═O intermediate, **4**. The quantum chemical results show that this species is better considered as Fe^{III}−O−Fe^{IV}−O•, having an unpaired electron on O, which gives the latter its very high reactivity, exceeding that of the P-450 ferryl group.

H atom abstraction (**4** → **5**) is rapidly followed by collapse of the transient methyl radical with the metal center via a weak Fe−CH_3 bond in structure **6**. The net apparent (2 + 2) addition process of **4** → **6** supports the prior proposals of Barton,[37] Baldwin,[38] Lippard,[39] and Dalton[40] for non-heme iron hydroxylation by this pathway, and the structure of **4** resembles the species proposed by Lipscomb[3b] and others.[41] Species **1**−**3** are far less reactive for H atom abstraction from CH_4 and are considered unlikely to be involved in this step. Direct OH abstraction by CH_3• (**5** → **7**) cannot be definitely excluded, but seems less likely. Finally, the loss of methanol leads to a Fe^{III}−OH−Fe^{III} dimer (**7**) that requires reduction to form the Fe_2(II,II) starting species. Comparison of the intermediates **1**−**6** with compounds **O** through **T**, found experimentally,[3] suggests tentative associations as follows: **1** compound **O**; **2**, **P**; **3**, **Q**; **4**, **R**; and **6**, **T**.

In addition to the work on the dinuclear species, results on a number of relevant mononuclear Fe(III) and Fe(IV) species are also reported. Fe(IV), a poorly understood oxidation state because its high reactivity prevents detailed study of stable species, presents an ideal opportunity for quantum chemical studies to delineate its structural chemistry and reactivity.

Although this is only a first reconnaissance into the theoretical aspects of this complex problem, we have at least suggested a detailed sequence of reactions that we hope will stimulate further experimental tests.

(36) Wilkins, P. C.; Dalton, H.; Podmore, I. D.; Deighton, N.; Symons, M. C. R. *Eur. J. Biochem.* **1992**, *210*, 67.

(37) Baldwin, J.; Adlington, R. M.; Flitsch, S. L.; Ting, H.-H.; Turner, N. J. *J. Chem. Soc., Chem. Commun.* **1986**, 1305.

(38) Barton, D. H. R.; Doller, D. *Acc. Chem. Res.* **1992**, *25*, 504. Barton, D. H. R.; Beviere, S. D.; Chavasiri, W.; Csushai, E.; Doller, D.; Liu, W.-G. *J. Am. Chem. Soc.* **1992**, *114*, 2147.

(39) Liu, K. E.; Johnson, C. C.; Newcomb, H., Lippard, S. J. *J. Am. Chem. Soc.* **1993**, *115*, 939.

(40) Wilkins, P. C.; Dalton, H.; Samuel, C. J.; Green, J. *Eur. J. Biochem.* **1994**, *226*, 555.

(41) Jaworska, M.; Rappe, A. K.; Gorun, S. M. *Inorg. Chem.* In press.

Note Added in Proof: EXAFS data on intermediate **Q** of the enzyme has recently been interpreted (Shu, L.; Nesheim, J. C.; Kauffmann, K.; Munck, E.; Lipscomb, J. D.; Que, L., Jr. *Science* **1997**, *275*, 515−517) in terms of an $Fe^{IV}-(\mu\text{-}O)_2-Fe^{IV}$ diamond core structure with asymmetric bridging oxo groups, essentially identical with the intermediate proposed here, and shown in Figure 3 and structure **3** in Figure 13. Que et al. have also synthesized a series of related model compounds, notably a $Fe^{III}-(\mu\text{-}O)_2-Fe^{III}$ structure: Que, L., Jr.; Dong, Y. *Acc. Chem. Res.* **1996**, *29*, 190−196.

JA963939M